ORGANOMETALLICS
Article
Cite This: Organometallics XXXX, XXX, XXX−XXX
pubs.acs.org/Organometallics

Probing the Influence of PAd-DalPhos Ancillary Ligand Structure on Nickel-Catalyzed Ammonia Cross-Coupling

Christopher M. Lavoie,[†] Joseph P. Tassone,[†] Michael J. Ferguson,[‡] Yuqiao Zhou,[‡] Erin R. Johnson,*[,†] and Mark Stradiotto*[,†]

[†]Department of Chemistry, Dalhousie University, 6274 Coburg Road, P.O. Box 15000, Halifax, Nova Scotia, Canada B3H 4R2
[‡]X-Ray Crystallography Laboratory, Department of Chemistry, University of Alberta, Edmonton, Alberta, Canada T6G 2G2

Supporting Information

ABSTRACT: We report herein on the results of our combined experimental/computational study regarding the catalytic performance of PAd-DalPhos (**L1**) in nickel-catalyzed ammonia arylation for primary aniline synthesis. Primary arylamine C−N reductive eliminations occurring from arylnickel(II) parent amido complexes of the type (**L**)Ni(Ph)(NH_2) were modeled by use of density-functional theory (DFT) methods, for a series of **L1** derivatives. The dual aims were to assess the effect of structural modifications to **L1** on potentially rate-limiting C−N reductive elimination and to identify promising candidates for experimental inquiry. Increasing the steric demand of the P_{aryl} groups from *o*-tolyl (in **L1**) to mesityl (in **L16**) resulted in a significant lowering of the barrier to C−N reductive elimination ($\Delta G^{‡}_{RE}$), which can be attributed in part to interactions between the ligand P_{aryl} groups and the nickel-bound amido ligand, as observed in noncovalent interaction (NCI) plots of the reductive elimination transition-state structures. Despite the favorability of **L16** predicted on the basis of computational analysis focusing on C−N reductive elimination, this ancillary ligand performed poorly in experimental testing versus **L1**, suggesting that in practice the significant steric demands of **L16** may discourage the formation of key catalytic intermediates. Modifications to the steric profile of the P_{aryl} groups in **L1** led to dramatic changes in catalytic performance, with the presence of an *o*-methyl proving to be important, among the **L1** variants tested, in achieving useful catalytic performance in the Ni-catalyzed monoarylation of ammonia.

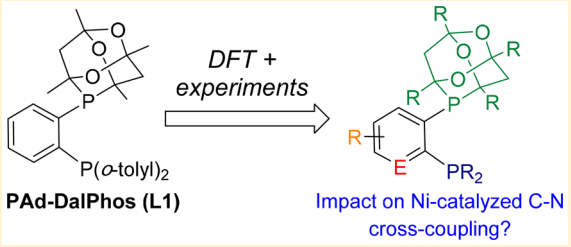

INTRODUCTION

The use of ammonia in transition-metal-catalyzed carbon−nitrogen (herein C−N) cross-coupling transformations involving inexpensive and abundant (hetero)aryl chlorides constitutes an attractive methodology for the production of primary arylamines, which are ubiquitous structural units found in a range of high-value chemicals (e.g., pharmaceuticals, agrochemicals, natural products, and beyond).[1−5] While appealing, the successful use of ammonia in cross-coupling methods is difficult to achieve on account of several salient challenges, which include, but are not restricted to, catalyst deactivation via ammonia-induced ancillary ligand dissociation,[6] slow C−N bond reductive elimination from sterically unencumbered parent amido intermediates,[7] and uncontrolled polyarylation of the initial primary arylamine product.[1,8] These challenges have largely been addressed in the domain of Pd-catalyzed C−N cross-coupling (i.e., Buchwald−Hartwig amination, BHA) through the application of optimally configured ancillary ligands (e.g., JosiPhos,[9] AdBrettPhos,[10] Mor-DalPhos,[11−13] BippyPhos,[14] and DiMeIHept^{Cl},[15] among others), which collectively give rise to palladium catalysts capable of effecting selective ammonia monoarylations with a useful spectrum of electrophiles, including (hetero)aryl chlorides.[16]

Recently there has been considerable progress made toward the development of complementary amination catalysts based on nickel.[17,18] If the catalysts are utilized in sufficiently low quantities (e.g., <5 mol %), such protocols can offer economic and other advantages over conventional BHA protocols based on palladium. To date, three ancillary ligands have emerged as being particularly effective in Ni-catalyzed ammonia monoarylation chemistry (**L1**−**L3**, Figure 1). In 2015 our group,[19] along with the Hartwig group,[20] independently reported on the first Ni-catalyzed ammonia monoarylations with (hetero)aryl chlorides for the synthesis of primary anilines (Figure 1)—a breakthrough that was enabled in both instances by the application of relatively electron rich, sterically bulky ferrocene-based JosiPhos ligands (**L2** and **L3**). In an effort to circumvent the use of expensive JosiPhos ligands, which are sold commercially as single enantiomers, we reported in 2016 on the development of the *o*-phenylene-bridged bidentate phosphine PAd-DalPhos (**L1**),[21] which, when employed in its (**L1**)NiCl(*o*-tolyl) precatalyst form, enables the C−N cross-coupling of a broad scope of (hetero)aryl (pseudo)halides with ammonia[21] and related NH reagents (e.g., primary alkylamines,[21] primary amides[22]) under mild reaction conditions.

Received: August 22, 2018

DOI: 10.1021/acs.organomet.8b00605
Organometallics XXXX, XXX, XXX−XXX

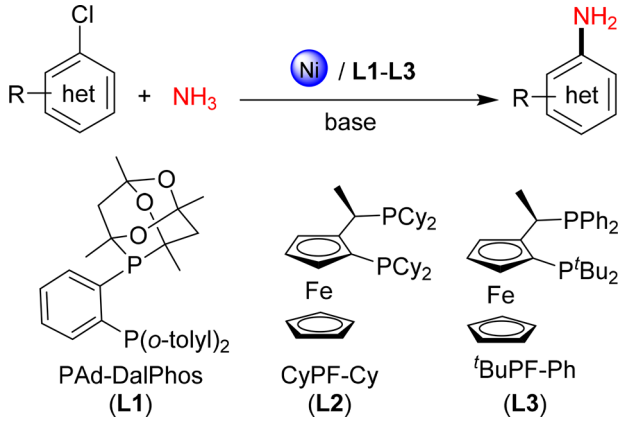

Figure 1. Prototypical nickel-catalyzed monoarylation of ammonia, involving the bisphosphine ancillary ligands **L1**–**L3**.

The key design features of **L1** (i.e., high steric demand, modestly electron-donating) were intended to facilitate ammonia monoarylation, given that such ancillary ligands might promote rate-limiting primary aniline C–N reductive elimination and discourage subsequent diarylation, within a presumptive Ni^0/Ni^{II} cycle.[23,24]

Given that only **L1**–**L3** are known to enable Ni-catalyzed ammonia monoarylations with demonstrated substrate scope, there exists a need for fundamental studies directed toward probing the influence of ancillary ligation on catalytic performance in such transformations. With this in mind, we sought to probe the effect on catalytic performance in Ni-catalyzed C–N cross-coupling reactions involving ammonia arising from structural modifications to **L1**, with the intention of leveraging new design concepts to inform the development of increasingly effective **L1** variants. In response, we have undertaken a combined computational and experimental investigation of Ni-catalyzed ammonia arylations, involving **L1** and related structural variants, which we disclose herein.

RESULTS AND DISCUSSION

We have previously evaluated complete catalytic cycles for Ni-catalyzed C–N cross-coupling reactions involving **L1** by use of density-functional theory (DFT) methods.[23,24] In all examined cases, these calculations predicted that, within a Ni^0/Ni^{II} cycle, C–N reductive elimination occurring from (**L**)Ni(aryl)(NHR) intermediates is rate limiting. As such, for the purposes of this study we explored the cross-coupling of chlorobenzene and ammonia to furnish aniline by use of DFT calculations, focusing exclusively on comparing ΔG°_{RE} and $\Delta G^\ddagger_{RE}$ values associated with aniline C–N reductive elimination from (**L**)Ni(Ph)(NH_2) (**IN-1**) intermediates via **TS-1** to afford (**L**)Ni(η^2-aniline) (**IN-2**) for each of PAd-DalPhos (**L1**) and its structural analogues (**L4**–**L16**; Figure 2). The variants of **L1** that we selected to examine featured the following structural modifications: extension of the phosphaadamantane (CgP) group alkyl chain length (**L4**), incorporation of phenylene backbone substituents (**L5**–**L7**), incorporation of heteroatoms into the backbone (**L8** and **L9**), and variation of the P_{aryl} substituents (**L10**–**L16**). The B3LYP-XDM[25–28] method and the 6-311+G(2d,2p) basis set were employed;[28] the geometry optimizations and frequency calculations were performed with a smaller mixed basis set, and frequencies were used to assign stationary points as either minima (no imaginary frequencies) or transition states (one imaginary frequency).

The computed ΔG°_{RE} and $\Delta G^\ddagger_{RE}$ values for the C–N reductive elimination of aniline from complexes of the type (**L**)Ni(Ph)(NH_2) (**IN-1**) are presented in Figure 2. The overall reaction (ΔG°_{RE}) is predicted to be thermodynamically favored for each of the examined **IN-1** variants, with the ΔG°_{RE} values spanning $-12.3 \leq \Delta G^\circ_{RE} \leq -1.7$ kcal mol^{-1}. Perhaps the most notable trend across the series is the observation that the computed free-energy barrier ($\Delta G^\ddagger_{RE}$) for **IN-1** species featuring the modeled ligands is influenced by the presence of *o*-methyl substitution on the P_{aryl} groups, as found in the parent ligand **L1**: relatively low barriers of ≤18.8 kcal mol^{-1} are calculated for **L1** variants featuring *o*-methyl substitution, whereas higher barriers (≥21.1 kcal mol^{-1}) are encountered in the absence of such substitution.

Our finding that the incorporation of *p*-fluoro substituents on the P(*o*-tolyl)$_2$ group in **L1** to give **L14** resulted in negligible variation of the ΔG°_{RE} and $\Delta G^\ddagger_{RE}$ values suggests that **L1** is relatively immune to such electronic perturbations. In exploring these ideas further, extension of the CgP alkyl length from Me to Et (**L4**), the addition of electronically and/or structurally varied substituents to the phenylene backbone (**L5**–**L7**), or incorporation of heteroaryl backbones in place of phenylene (**L8** and **L9**) each had a minimal effect on the $\Delta G^\ddagger_{RE}$ values (all within 0.4 kcal mol^{-1} of **IN-1** featuring **L1**). The ΔG°_{RE} values arising from **IN-1** complexes featuring the (aryl)P(*o*-tolyl)$_2$ type ligands **L4**–**L9** were found to be somewhat more varied, with the 3,4-substituted thiophene version (**L9**) in particular predicted to afford a significantly more exergonic C–N reductive elimination (ΔG°_{RE} = −12.3 kcal mol^{-1}) in comparison to the other **IN-1** variants. While we are currently unsure as to the specific origins of the differing ΔG°_{RE} values arising from **IN-1** complexes featuring **L1** (PAd-DalPhos) or **L9** (ThioPAd-DalPhos), we have observed that, in selected Ni-catalyzed C–N cross-coupling applications involving primary alkylamines under low-loading conditions, the performance of **L9** is indeed superior to that of **L1**.[29]

In examining C–N reductive elimination from **IN-1** species featuring exclusively meta- or para-substituted P_{aryl} groups (e.g., **L10**–**L13**), or a simple (aryl)PPh_2 donor unit (PhPAd-DalPhos, **L15**), a minimal effect on $\Delta G^\ddagger_{RE}$ was noted; however, such modifications resulted in some modest changes to ΔG°_{RE}, as seen in the comparison of **L10** (ΔG°_{RE} = −1.7 kcal mol^{-1}) and **L11** (ΔG°_{RE} = −5.6 kcal mol^{-1}). Given the apparent benefits of the P(*o*-tolyl)$_2$ moiety in **L1**, we speculated that related ancillary ligand variants featuring di-*o*-methyl substitution might give rise to even lower $\Delta G^\ddagger_{RE}$ values. Consistent with this hypothesis, replacement of the P(*o*-tolyl)$_2$ moiety in **L1** with a sterically demanding dimesitylphosphino (i.e., $PMes_2$) donor group (**L16**) led to a significant reduction in the calculated $\Delta G^\ddagger_{RE}$ value from the related **IN-1** species (16.4 versus 18.6 kcal mol^{-1} for **L16** and **L1**, respectively), as depicted in Figure 2.

In an effort to gain further insight into the potential role of P_{aryl} steric contributions to the observed difference in $\Delta G^\ddagger_{RE}$ values calculated for **IN-1** complexes featuring **L1** and its structural analogues, we generated noncovalent interaction (NCI) plots for the C–N reductive elimination transition-state species (**TS-1**) based on **L1**, **L15**, and **L16** (Figure 3). NCI plots provide a convenient visualization of inter- and intramolecular interactions in real space.[30] These are generated by plotting the isosurface of the reduced density gradient for a defined region of space; the resulting colored isosurfaces indicate regions in space wherein the electron densities of

DOI: 10.1021/acs.organomet.8b00605
Organometallics XXXX, XXX, XXX–XXX

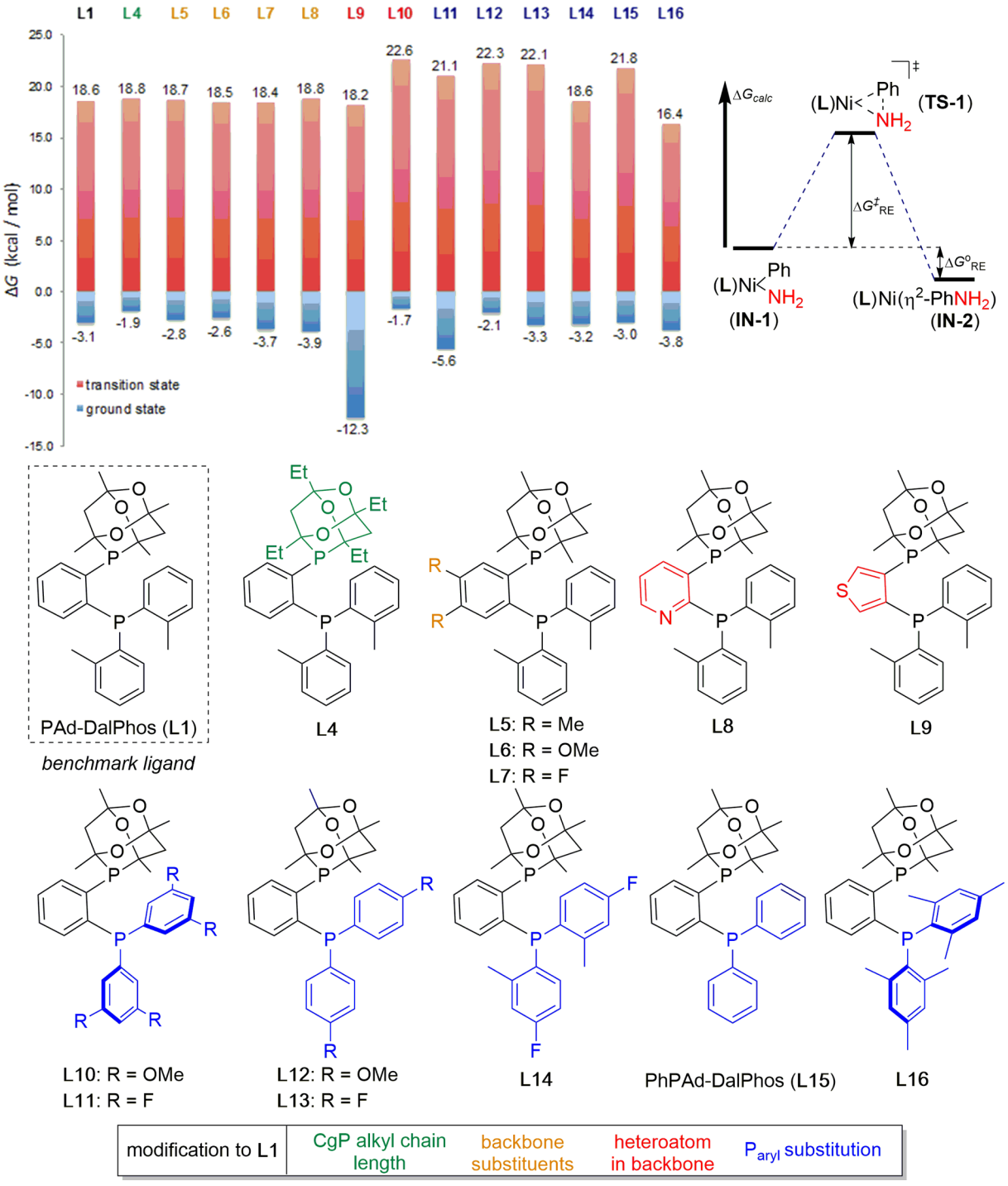

Figure 2. Computed ΔG°_{RE} (blue) and $\Delta G^{\ddagger}_{RE}$ (red) values associated with aniline C–N reductive elimination from (**L**)Ni(Ph)(NH_2) (**IN-1**) involving **L1** and structural analogues (**L4**–**L16**).

different domains of the ligand are interacting in a noncovalent manner (e.g., steric repulsion, π–π stacking, van der Waals interactions). The major NCI features of the defined region of the **L1**-derived transition state are CH–π interactions between the CH_3 groups of the CgP unit and the Ni-bound phenyl ligand and interactions between the *o*-methyl group of the P_{aryl} fragment and the Ni-bound amido ligand. While the CH–π interactions observed in the **L1**-based transition state are present in both the **L15**- and **L16**-derived **TS-1** structures, there are no significant interactions between the Ni-bound amido group and the phenyl groups on **L15**, whereas interactions of this type are present in the **L16**-based transition-state structure. The observation that the NCI data correlate with the calculated $\Delta G^{\ddagger}_{RE}$ values (**L15** > **L1** > **L16**) highlights the benefits of steric loading on the P_{aryl} groups of **L1** ancillary ligand variants as a means of promoting C–N reductive elimination. Schoenebeck and co-workers[31] recently exploited this effect in achieving Pd-centered Ph–CF_3 reductive elimination by utilizing a CF_3-substituted bis(diphenylphosphino)ethane (dppe) ancillary ligand, which induces ground-state destabilization and thus a lowering of the transition-state barrier via electrostatic repulsion of the

DOI: 10.1021/acs.organomet.8b00605
Organometallics XXXX, XXX, XXX–XXX

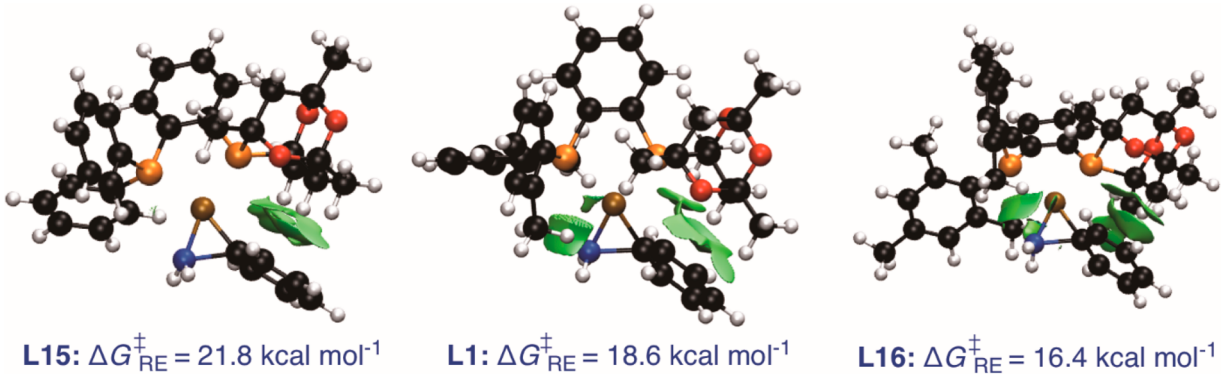

Figure 3. Noncovalent interaction (NCI) isosurfaces for **TS-1** structures featuring **L1**, **L15**, and **L16**. Atom colors: Ni (brown), C (black), H (white), O (red), P (orange), N (blue).

bisphosphine ancillary ligand and the reacting phenyl and CF_3 groups.

Our computational analyses indicated that the more sterically demanding **L16**, which exhibits a relatively low barrier for C−N reductive elimination, might give rise to more efficient ammonia monoarylation chemistry relative to **L1** and **L15**, assuming that arylnickel(II) parent amido intermediates of the type (**L**)Ni(Ph)NH_2 are accessed in a comparable manner for these ligands. We sought to test this assertion experimentally by comparing the catalytic behavior of nickel complexes supported by each of **L1**, **L15**, and **L16** in C−N cross-coupling test reactions involving ammonia and aryl chlorides. The new bisphosphine **L16** was prepared in a manner analogous to that used for the synthesis of **L1**[21] and was fully characterized on the basis of NMR spectroscopy and high-resolution mass spectrometric data and by the use of X-ray crystallographic techniques (Figure 4).

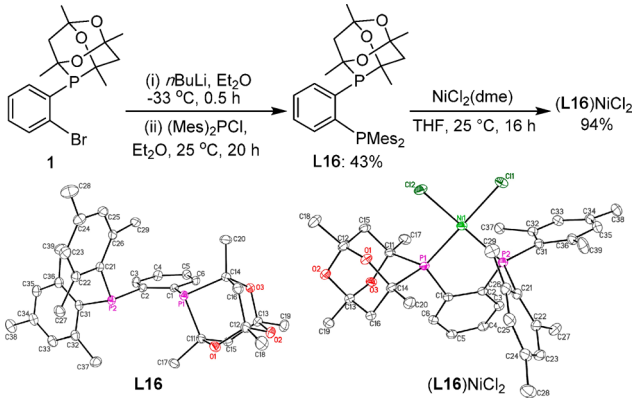

Figure 4. Synthesis and single-crystal X-ray structures of **L16** and (**L16**)$NiCl_2$, represented with thermal ellipsoids at the 30% probability level and with hydrogen atoms omitted for clarity. Selected interatomic distances (Å) and angles (deg) for (**L16**)$NiCl_2$: Ni−P1 2.1902(6); Ni−P2 2.1738(6); Ni−Cl1 2.2135(6); Ni−Cl2 2.1840(6), P1−Ni−P2 88.06(2). dme = 1,2-dimethoxyethane.

In a preliminary effort to assess the relative catalytic performances of catalysts based on **L1**, **L15**, and **L16**, we conducted Ni-catalyzed C−N test cross-couplings involving 4-chlorobiphenyl (**2**) and ammonia to furnish 4-aminobiphenyl (**A**), employing 5 mol % each of ligand and $Ni(cod)_2$, under conditions we had established in a prior report.[21] Monitoring the consumption of **2** over time (see Figure S1 in the Supporting Information) revealed that **L1**/$Ni(cod)_2$ catalyst mixtures were the most active, with complete conversion of **2** being observed after only 30 min. While our observation that the less hindered **L15** variant gave rise to slower turnover relative to **L1** was expected on the basis of their calculated $\Delta G^{\ddagger}_{RE}$ values (**L1**, 18.6 kcal mol^{-1}; **L15**, 21.8 kcal mol^{-1}), the comparatively modest consumption of **2** (ca. 20% conversion after 30 min) when **L16**/$Ni(cod)_2$ catalyst mixtures were employed was not anticipated. Furthermore, the computed barriers to C−Cl oxidative addition occurring from intermediates of the type (**L**)Ni(η^2-PhCl) are comparatively low for both **L1** (7.2 kcal mol^{-1})[23] and **L16** (7.9 kcal mol^{-1}), indicating that the difference in observed activity is not likely the result of slow oxidative addition in the case of **L16**. We speculated that inefficient substitution of a diene ligand in $Ni(cod)_2$ by the sterically encumbered **L16** might explain in part its inferior activity. To examine this hypothesis, we prepared 1:1 mixtures of each of **L1**, **L15**, or **L16** and $Ni(cod)_2$ in C_6D_6 (2 h, 80 °C) and monitored the formation of putative (**L**)Ni(cod) species by use of $^{31}P\{^1H\}$ NMR analysis (Scheme 1); a structurally related 1,1′-bis(diphenylphosphino)ferrocene (dppf)-based (**L**)Ni(cod) complex was recently characterized by use of X-ray crystallographic techniques.[32] Whereas **L1** and **L15** each gave rise to partial (**L1**) or complete (**L15**) conversion to the putative (**L**)Ni(cod) species, only free ligand was detected in the case of **L16**. Collectively these observations confirm that, while **L16** may indeed be efficient in promoting reductive elimination from **IN-1** type inter-

Scheme 1. Extent of Ligand Substitution Reactions between L1, L15, or L16 and $Ni(cod)_2$ on the Basis of $^{31}P\{^1H\}$ NMR Spectroscopic Data[a]

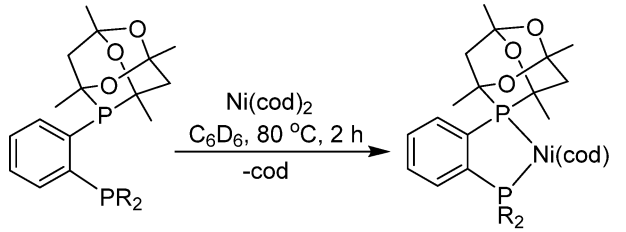

L1 (R = *o*-tolyl)
L15 (R = Ph)
L16 (R = Mes)

L1: ~50% conversion
L15: >95% conversion
L16: <5% conversion

[a]cod = 1,5-cyclooctadiene.

DOI: 10.1021/acs.organomet.8b00605
Organometallics XXXX, XXX, XXX−XXX

mediates when they are formed, the significant steric demands of this ancillary ligand may lead to inefficient formation of requisite ligated precatalyst species (e.g., formation of precatalyst (**L16**)Ni(cod) from Ni(cod)$_2$ in situ).

In light of the poor reactivity observed between Ni(cod)$_2$ and **L16**, we turned our attention to the synthesis of an (**L16**)NiCl(*o*-tolyl) precatalyst.[33] Such precatalysts routinely outperform **L**/Ni(cod)$_2$ mixtures by virtue of avoiding potentially inhibiting cod[32,34] and by offering ancillary ligand precoordination to nickel. Treatment of NiCl$_2$(dme) with each of **L1**, **L15**, and **L16** resulted in the clean formation of the target (**L**)NiCl$_2$ complexes; the X-ray structure of (**L16**)NiCl$_2$ is presented in Figure 4. Treatment of (**L16**)NiCl$_2$ with (*o*-tolyl)MgCl under established conditions[21] resulted in the formation of a new product exhibiting two resonances appearing at 53.4 and 29.0 ppm (J_{PP} = 11.2 Hz) in the $^{31}P\{^1H\}$ NMR spectrum of the crude reaction mixture, which we tentatively assign to the target (**L16**)NiCl(*o*-tolyl) complex. Unfortunately, attempts to isolate pure material from such reactions led to decomposition of the putative target complex into unidentified paramagnetic impurities. Given the apparent complexity associated with the synthesis of (**L16**)NiCl(*o*-tolyl), in moving forward we opted to employ (**L**)NiCl$_2$/(*o*-tolyl)MgCl mixtures to achieve formation of the desired (**L**)NiCl(*o*-tolyl) catalyst precursor in situ; proof of principle experimentation comparing the catalytic performances of preformed (**L1**)NiCl(*o*-tolyl) and (**L1**)NiCl$_2$/(*o*-tolyl)MgCl mixtures demonstrated the viability of this approach (see GP3 of the Experimental Section for details).

We began our reactivity survey by examining the effect of ammonia concentration on the selectivity of the (**L1**)NiCl$_2$/(*o*-tolyl)MgCl-based amination of 4-chlorobiphenyl (**2**) with ammonia (0.5 M in 1,4-dioxane) to produce 4-aminobiphenyl (**A**) and potentially bis(4-biphenylyl)amine (**B**). Using (**L1**)NiCl$_2$ (5 mol %), (*o*-tolyl)MgCl (0.2 equiv), sodium *tert*-butoxide (2.0 equiv) as the base, and ammonia (10 equiv) relative to **2**, resulted in complete conversion of **2** at 110 °C and relatively good selectivity for **A** (Scheme 2, entry 4). Decreasing the amount of ammonia (3 or 7 equiv), while the concentration of **2** was kept the same, resulted in only a moderate decrease in the yield of **A** (Scheme 2, entries 2 and 3); however, modestly better selectivity was observed when 7 equiv of ammonia versus 3 equiv was used. Utilizing 1 equiv of ammonia led to incomplete conversion of **2**, negligible quantities of **A**, and significant formation of **B** (Scheme 2, entry 1). The trend of increased ammonia concentration leading to improved monoarylation selectivity can likely be attributed to an increase in the ratio of (**L1**)Ni(aryl)(NH$_2$) to (**L1**)Ni(aryl)(NHaryl) intermediates, given that both ammonia and the monoarylation product **A** are competing substrates.

Scheme 2. Ancillary Ligand Screen in the Nickel-Catalyzed C−N Cross-Coupling of 4-Chlorobiphenyl (2) with Ammonia[a]

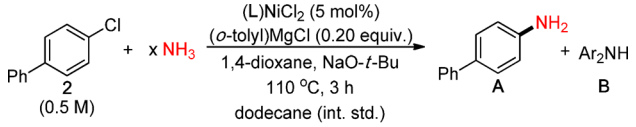

Entry	Ligand	NH_3 equiv.	% 2	% Yield A	% Yield B	A / B
1	**L1**	1	48	<3	27	-
2	**L1**	3	<3	72	15	4.8
3	**L1**	7	<3	72	9	9
4	**L1**	10	<3	81	8	10.1
5	**L15**	10	<3	<3	36	-
6	**L16**	10	<3	12	37	0.3
7	**L2**	10	<3	88	3	29.3

[a]Quantities of **2**, **A**, and **B** were calculated on the basis of calibrated GC data, using dodecane and authentic products as internal standards.

Having identified optimized conditions for achieving selectivity for **A** with precatalyst (**L1**)NiCl$_2$ (i.e., Scheme 2, entry 4), we then examined the reactivity profile of related (**L**)NiCl$_2$ precatalysts featuring **L15** and **L16**. While full consumption of **2** was observed in both cases (Scheme 2, entries 5 and 6), the diarylated product **B** was obtained as the major product. Having shown **L1** to be superior to both **L15** and **L16** in this application, we subsequently probed the catalytic abilities of the analogous JosiPhos precatalyst (**L2**)NiCl$_2$[19] to provide a comparison of what can be viewed as the two most highly effective ligands known for Ni-catalyzed ammonia arylations: CyPF-Cy (**L2**)[19,35−37] and PAd-DalPhos (**L1**).[18,21,37] Use of (**L2**)NiCl$_2$/(*o*-tolyl)MgCl catalyst mixtures under our optimized conditions resulted in the consumption of **2** and somewhat improved selectivity for **A** over **B** (Scheme 2, entry 7), relative to that achieved by use of (**L1**)NiCl$_2$/(*o*-tolyl)MgCl (Scheme 2, entry 4).

In an effort to better understand the diverse reactivity profiles exhibited by each of the (**L**)NiCl$_2$ precatalysts examined above (**L** = **L1**, **L2**, **L15**, **L16**), we monitored the reaction mixture product distribution at various time intervals throughout the course of catalytic experiments. Precatalysts (**L1**)NiCl$_2$ and (**L2**)NiCl$_2$ gave rise to the fastest consumption of **2**, with each achieving full conversion within 60 min (see Figure S2 in the Supporting Information). This was accompanied in both cases by a steady increase in the yield of primary arylamine **A** (Figure 5) and minimal formation

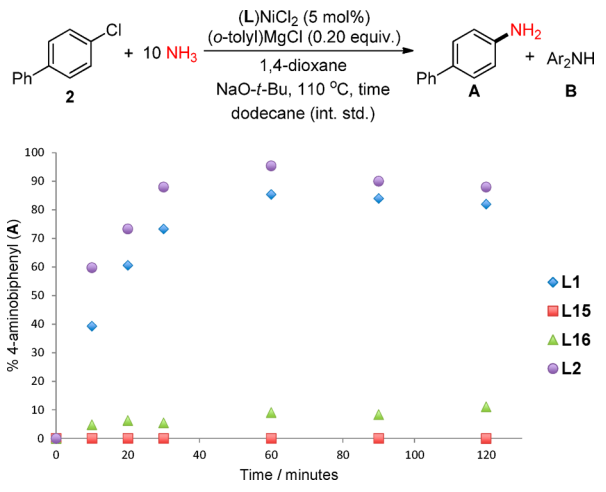

Figure 5. Time course for the conversion of **2** into 4-aminobiphenyl (**A**) using (**L**)NiCl$_2$/(*o*-tolyl)MgCl catalyst mixtures. See GP4 of the Experimental Section for details.

(<10%) of diarylated **B** (see Figure S3 in the Supporting Information). Precatalysts (**L15**)NiCl$_2$ and (**L16**)NiCl$_2$ gave rise to comparatively slow consumption of **2**, with each requiring 120 min to achieve full conversion (see Figure S2). Despite substantial quantities of secondary arylamine **B** being formed throughout the reaction (see Figure S3), the amount of primary arylamine **A** detected was consistently low (<15%;

DOI: 10.1021/acs.organomet.8b00605
Organometallics XXXX, XXX, XXX−XXX

Figure 5), indicating that the uptake of initially formed **A** is likely rapid for catalyst systems featuring **L15** or **L16**. For ligand-specific time course data, see Figures S4–S7 in the Supporting Information.

Whereas the poor monoarylation selectivity observed in Ni-catalyzed ammonia C–N cross-couplings involving the comparatively unhindered **L15** can be attributed to facile coordination/arylation of the initially formed primary aniline **A**, a similar rationale for the low conversion and monoarylation selectivity observed when the hindered **L16** variant was used would not seem to be applicable.

In testing the ability of the (**L**)$NiCl_2$ precatalysts herein to enable primary arylamine arylations, we examined the cross-coupling of **2** (1.0 equiv) with 4-aminobiphenyl (**A**; 1.0 equiv) to furnish bis(4-biphenylyl)amine (**B**) under conditions similar to those outlined in Scheme 2, but in the absence of ammonia (Figure S8 in the Supporting Information). The use of (**L15**)$NiCl_2$/(*o*-tolyl)MgCl catalyst mixtures resulted in the formation of substantial quantities of **B** (76%, Figure S8, entry 2), which is consistent with the proposal that a less hindered coordination environment allows for facile primary arylamine coordination and thus decreased monoarylation selectivity in ammonia cross-couplings. In contrast, comparatively low consumption of **2** and **A** (29–41%) and poor formation of **B** (20–23%) was achieved by use of precatalysts based on **L1**, **L2**, and **L16** (Figure S8, entries 1, 3, and 4). The poor reactivity (<5% consumption of **2**) exhibited by $NiCl_2$(dme)/(*o*-tolyl)MgCl catalyst mixtures suggests that nickel species lacking phosphine ligation are unlikely to contribute significantly to the observed reactivity of (**L16**)$NiCl_2$/(*o*-tolyl) catalyst mixtures. Collectively, these observations reveal **L16** to be a relatively ineffective ligand for use in nickel-catalyzed C–N cross-couplings of ammonia or the primary arylamine **A** with electrophile **2**, despite the low barrier ($\Delta G^{\ddagger}_{RE}$) for C–N reductive elimination predicted for the **IN-1** species featuring κ^2-**L16** (Figure 2). In this regard, it is possible that under catalytic conditions **L16** does not bind as a κ^2-bisphosphine ligand, despite crystallographic support for such connectivity in the precatalyst (**L16**)$NiCl_2$ (Figure 4).

CONCLUSIONS

In an effort to better understand the desirable catalytic performance of PAd-DalPhos (**L1**) in the Ni-catalyzed monoarylation of ammonia, and to guide the development of increasingly effective variants of **L1**, we conducted a combined experimental/computational study, the results of which we have reported herein. In computationally modeling C–N reductive eliminations occurring from arylnickel(II) parent amido complexes of the type (**L**)Ni(Ph)(NH_2), one key observation was that increasing the steric demand of the P_{aryl} groups from *o*-tolyl (in **L1**) to mesityl (in **L16**) resulted in a significant lowering of the barrier to C–N reductive elimination ($\Delta G^{\ddagger}_{RE}$). However, empirically the newly prepared **L16** performed poorly versus **L1**, suggesting that the significant steric demands of **L16** may discourage formation of key catalytic intermediates. Conversely, the poor monoarylation selectivity afforded by the **L1** variant featuring a PPh_2 donor fragment (**L15**) can be attributed to facile coordination/arylation of the initially formed primary aniline. Collectively these observations suggest that the intermediate steric profile of **L1**, relative to **L15** and **L16**, may be optimal in achieving useful catalytic performance in the Ni-catalyzed monoarylation of ammonia. Our current work is focused on developing new ancillary ligand variants that adhere to these design principles for application in challenging Ni-catalyzed cross-couplings. We will report on the outcome of these studies in due course.

EXPERIMENTAL SECTION

General Considerations. Unless otherwise stated, all reactions were set up inside a nitrogen-filled inert atmosphere glovebox using oven-dried glassware and purified solvents and were worked up in air using benchtop procedures. Toluene and hexanes were dried/deoxygenated by sparging with nitrogen, followed by passage through a double-column solvent purification system packed with alumina and copper-Q5 reactant, and stored over activated 4 Å molecular sieves. 1,4-Dioxane was dried over Na/benzophenone followed by distillation under a nitrogen atmosphere. Deuterated NMR solvents were freeze–pump–thaw degassed three times followed by storage over activated 4 Å molecular sieves. **1**, **L1** (PAd-DalPhos), and **L15** (PhPAd-DalPhos) were each synthesized according to an existing literature procedure.[21] Precatalysts (**L**)$NiCl_2$ (**L** = **L1**, **L2**) were synthesized following literature procedures.[19,21] All other commercial solvents, reagents, and materials were used as received. NMR spectra were recorded on a Bruker AV 300 MHz or Bruker AV 500 MHz spectrometer at 300 K, with chemical shifts (in ppm) referenced to residual protio solvent peaks (^1H), deuterated solvent peaks ($^{13}C\{^1H\}$), or external 85% H_3PO_4 in D_2O ($^{31}P\{^1H\}$). Mass spectra were obtained using ion trap electrospray ionization (ESI) instruments operating in positive mode. Gas chromatography data were obtained on an instrument equipped with an SGE BP-5 column (30 m, 0.25 mm i.d.), and were response factor calibrated with authentic materials using dodecane as an internal standard.

General Procedure for Monitoring the Reaction Progress for the Cross-Coupling of Ammonia and 4-Chlorobiphenyl Using L/Ni(cod)$_2$ Mixtures (GP1). *Individual reactions were set up for each time interval.* In a nitrogen-filled glovebox, bis(cyclooctadiene)-nickel(0) (1.7 mg, 0.006 mmol, 0.05 equiv), ligand (0.006 mmol, 0.05 equiv), 4-chlorobiphenyl (**2**; 22.6 mg, 0.12 mmol, 1.0 equiv), sodium *tert*-butoxide (34.6 mg, 0.36 mmol, 3.0 equiv), ammonia as a 0.5 M solution in 1,4-dioxane (1.2 mL, 0.6 mmol, 5.0 equiv), and toluene (0.466 mL; [ArCl] = 0.072 M) were placed in a screw-capped vial containing a magnetic stir bar. The vial was sealed with a cap containing a PTFE septum, removed from the glovebox, and placed in a temperature-controlled aluminum heating block set to 110 °C with magnetic stirring. At the designated time, the reaction vial was removed from the heating block and left to cool to ambient temperature, followed by addition of dodecane internal standard (0.12 mmol, 1.0 equiv) to the reaction mixture, which was subsequently analyzed by use of GC methods following **Workup Method A**.

General Procedure for the Cross-Coupling of Ammonia and 4-Chlorobiphenyl Using (L)$NiCl_2$/(*o*-tolyl)MgCl Mixtures (GP2). In a nitrogen-filled glovebox, (**L**)$NiCl_2$ precatalyst (0.006 mmol, 5 mol %), 4-chlorobiphenyl (22.6 mg, 0.12 mmol, 1.0 equiv), sodium *tert*-butoxide (23.1 mg, 0.24 mmol, 2.0 equiv), *o*-tolylmagnesium chloride as a 1.0 M solution in THF (24.0 μL, 0.024 mmol, 0.2 equiv), and ammonia as a 0.5 M solution in 1,4-dioxane (0.24–2.40 mL, 0.12–1.2 mmol, 1–10 equiv), were placed in a screw-capped vial containing a magnetic stir bar, followed by the addition of 1,4-dioxane to give [ArCl] = 0.05 M. The vial was sealed with a cap containing a PTFE septum, removed from the glovebox, and placed in a temperature-controlled aluminum heating block set to 110 °C with magnetic stirring. At the designated time, the reaction vial was removed from the heating block and left to cool to ambient temperature, followed by addition of dodecane internal standard (0.12 mmol, 1.0 equiv) to the reaction mixture, which was subsequently analyzed by use of GC methods following **Workup Method A**.

General Procedure for the Cross-Coupling of Ammonia and 4-Chlorobiphenyl Using the (L1)NiCl(*o*-tolyl) Precatalyst (GP3). In a nitrogen-filled glovebox, precatalyst (0.006 mmol, 5 mol %), 4-chlorobiphenyl (**2**; 22.6 mg, 0.12 mmol, 1.0 equiv), sodium *tert*-butoxide (23.1 mg, 0.24 mmol, 2.0 equiv), and ammonia as a 0.5 M solution in 1,4-dioxane (2.4 mL, 1.2 mmol, 10.0 equiv) were placed in a screw-capped vial containing a magnetic stir bar. The vial was

DOI: 10.1021/acs.organomet.8b00605
Organometallics XXXX, XXX, XXX–XXX

sealed with a cap containing a PTFE septum, removed from the glovebox, and placed in a temperature-controlled aluminum heating block set to 110 °C with magnetic stirring. At the designated time, the reaction vial was removed from the heating block and left to cool to ambient temperature, followed by addition of dodecane internal standard (0.12 mmol, 1.0 equiv) to the reaction mixture, which was subsequently analyzed by use of GC methods following **Workup Method A**. The product distribution observed when this method was used (<5% unreacted ArCl, 71% $ArNH_2$, 11% Ar_2NH) is similar to that observed for analogous reactions employing (**L1**)$NiCl_2$/(*o*-tolyl)MgCl catalyst mixtures (**GP2**) (<5% unreacted ArCl, 81% $ArNH_2$, 8% Ar_2NH).

General Procedure for Monitoring the Reaction Progress for the Cross-Coupling of Ammonia and 4-Chlorobiphenyl Using (L)$NiCl_2$/(*o*-tolyl)MgCl Mixtures (GP4). *Individual reactions were set up for each time interval.* In a nitrogen-filled glovebox, precatalyst (0.006 mmol, 5 mol %), 4-chlorobiphenyl (**2**; 22.6 mg, 0.12 mmol, 1.0 equiv), sodium *tert*-butoxide (23.1 mg, 0.24 mmol, 2.0 equiv), *o*-tolylmagnesium chloride as a 1.0 M solution in THF (24.0 μL, 0.024 mmol, 0.2 equiv), and ammonia as a 0.5 M solution in 1,4-dioxane (2.4 mL, 1.2 mmol, 10.0 equiv) were placed in a screw-capped vial containing a magnetic stir bar. The vial was sealed with a cap containing a PTFE septum, removed from the glovebox, and placed in a temperature-controlled aluminum heating block set to 110 °C with magnetic stirring. At the designated time, the reaction vial was removed from the heating block and left to cool to ambient temperature, followed by addition of dodecane internal standard (0.12 mmol, 1.0 equiv) to the reaction mixture, which was subsequently analyzed by use of GC methods following **Workup Method A**.

General Procedure for the Cross-Coupling of 4-Aminobiphenyl and 4-Chlorobiphenyl Using (L)$NiCl_2$/(*o*-tolyl)MgCl Mixtures (GP5). In a nitrogen-filled glovebox, precatalyst (0.006 mmol, 5 mol %), 4-chlorobiphenyl (**2**; 22.6 mg, 0.12 mmol, 1.0 equiv), sodium *tert*-butoxide (23.1 mg, 0.24 mmol, 2.0 equiv), *o*-tolylmagnesium chloride as a 1.0 M solution in THF (24.0 μL, 0.024 mmol, 0.2 equiv), and 4-aminobiphenyl (20.3 mg, 0.12 mmol, 1.0 equiv) were placed in a screw-capped vial containing a magnetic stir bar, followed by the addition of 2.4 mL of 1,4-dioxane ([ArCl] = 0.05 M). The vial was sealed with a cap containing a PTFE septum, removed from the glovebox, and placed in a temperature-controlled aluminum heating block set to 110 °C for 2 h with magnetic stirring. The reaction vial was then removed from the heating block and left to cool to ambient temperature, followed by addition of dodecane internal standard (0.12 mmol, 1.0 equiv) to the reaction mixture, which was subsequently analyzed by use of GC methods following **Workup Method A**.

Workup Method A: Procedure for the Preparation of GC Samples. Following **GP1**−**GP5**, the reaction mixture was diluted using ethyl acetate and was passed through a Kimwipe filter containing Celite and silica. The eluent was collected in a GC vial, followed by analysis using calibrated GC methods.

General Procedure for Ligand Substitution Reactions Involving L and Ni(cod)$_2$ (Scheme 1). In a nitrogen-filled glovebox, **L1**, **L15**, or **L16** (0.019 mmol), and bis(cyclooctadiene)-nickel(0) (5.2 mg, 0.019 mmol) were placed in a screw-capped vial containing a magnetic stir bar, followed by the addition of 0.75 mL of C_6D_6. The vial was sealed with a cap containing a PTFE septum and placed in a temperature-controlled aluminum heating block set to 80 °C for 2 h with magnetic stirring. After the mixture was cooled to ambient temperature, the vial was brought into the glovebox and an NMR sample was prepared. Analysis of the reaction mixture by use of $^{31}P\{^1H\}$ NMR methods revealed partial conversion of **L1** and the appearance of two resonances at 46.1 and 38.4 ppm (J_{PP} = 40.5 Hz), which we tentatively assign to (**L1**)Ni(cod). For **L15**, analysis of the reaction mixture by use of $^{31}P\{^1H\}$ NMR methods revealed complete consumption of **L15** and the appearance of two resonances at 51.2 and 38.5 ppm (J_{PP} = 40.5 Hz), which we tentatively assign to (**L15**)Ni(cod). For **L16**, only free ligand was detected upon analysis of the reaction mixture by use of $^{31}P\{^1H\}$ NMR methods.

Synthesis of L16. In a nitrogen-filled glovebox, **1** (0.400 g, 1.08 mmol, 1.0 equiv) and diethyl ether (ca. 6 mL) were combined in a 4 dram vial along with a magnetic stir bar. The vial was sealed and then cooled to −33 °C in the glovebox freezer. This vial was then removed from the freezer, and a 2.5 M hexanes solution of cold (−33 °C) *n*-butyllithium (0.517 mL, 1.3 mmol, 1.2 equiv) was added dropwise under the influence of magnetic stirring, resulting in a yellowish orange solution. This mixture was stirred for 30 min at ambient temperature. At this time, a solution of dimesitylphosphorus chloride (395.0 mg, 1.3 mmol, 1.2 equiv) in diethyl ether (ca. 6 mL) was added, resulting in an orange solution. This mixture was stirred at ambient temperature for 20 h. On the benchtop, the reaction mixture was diluted with CH_2Cl_2 (ca. 10 mL) and filtered over Celite, with CH_2Cl_2 as eluent (ca. 20 mL). The eluent was collected, and the solvent was removed via rotary evaporation. The resulting yellow oil was purified by flash chromatography (SiO_2), with 3% ethyl acetate/hexanes as eluent. The resulting beige waxy solid was recrystallized in cold pentane (0 °C) overnight, which following filtration afforded **L16** as a white crystalline solid (260.0 mg, 43% yield). ^1H NMR ($CDCl_3$, 500.1 MHz): δ 8.27 (m, 1H, ArH), 7.30−7.27 (m, 1H, ArH), 7.17−7.13 (m, 2H, ArH), 6.90 (d, *J* = 2.0 Hz, 2H, ArH), 6.76 (d, *J* = 2.5 Hz, 2H, ArH), 2.31 (s, 3H, Me), 2.27 (s, 3H, Me), 2.16−2.13 (m, 7H, Me/CgP), 2.04−2.02 (m, 7H, Me/CgP), 1.89 (m, 1H, CgP), 1.59−1.55 (m, 4H, CgP), 1.48 (s, 3H, Me), 1.39 (s, 3H, Me), 1.38 (d, *J* = 12.0 Hz, 3H, Me). $^{13}C\{^1H\}$ NMR ($CDCl_3$, 125.8 MHz): δ 148.1 (dd, *J* = 33.9, 15.1 Hz, ArC), 144.5 (d, *J* = 16.3 Hz, ArC), 142.3 (d, *J* = 16.3 Hz, ArC), 140.7−140.2 (m, ArC), 138.8 (ArC), 137.3 (ArC), 134.1 (ArC), 133.4 (d, *J* = 7.5 Hz, ArC), 131.8 (d, *J* = 18.9 Hz, ArC), 130.8 (dd, *J* = 20.7, 11.3 Hz, ArC), 130.2 (dd, *J* = 35.2, 3.8 Hz, ArC), 129.4 (ArC), 128.1 (ArC), 97.0 (CgP), 96.2 (CgP), 74.7−74.3 (m, CgP), 46.2 (d, *J* = 20.1 Hz, CgP), 36.5 (CgP), 29.1 (dd, *J* = 18.9, 7.5 Hz, CgP), 28.4 (Me), 27.9 (Me), 26.8 (d, *J* = 11.3 Hz, Me), 23.6 (dd, *J* = 41.5, 16.3 Hz, Me), 21.2 (d, *J* = 10.0 Hz, Me). $^{31}P\{^1H\}$ (202.5 MHz, $CDCl_3$): δ −24.9 (d, J_{PP} = 158 Hz, 1P), −36.8 (d, J_{PP} = 159 Hz, 1P). HRMS-ESI (*m*/*z*): calcd for $C_{34}H_{43}O_3P_2$ [M + H], 561.2687; found, 561.2682. A single crystal suitable for X-ray diffraction was obtained by slow evaporation of **L16** in cold (0 °C) hexanes.

Synthesis of (L15)$NiCl_2$. In a nitrogen-filled glovebox, a 4 dram vial was charged with $NiCl_2$(dme) (219.6 mg, 0.999 mmol, 1.0 equiv) and **L15** (500.0 mg, 1.05 mmol 1.05 equiv). To these solids was added THF (ca. 10 mL), affording a cloudy brown mixture. A magnetic stir bar was added, the vial was sealed, and stirring was initiated. After several minutes, a red precipitate formed. The resulting mixture was stirred at ambient temperature for 2 h, after which time the vial was removed from the glovebox and pentane (5 mL) was added. The precipitated red solid was collected on a glass filter frit, and the retained solid was washed with cold (∼0 °C) pentane (3 × 3 mL). The collected solid product was then washed off of the frit by passing CH_2Cl_2 (ca. 50 mL) through the frit, followed by evaporation of solvent from the intensely red eluent. The product was then dried in vacuo to afford the desired complex as a crimson solid (520 mg, 86%). ^1H NMR (500.1 MHz, $CDCl_3$): δ 8.45 (d, *J* = 8.0 Hz, 1H, ArH), 8.04 (d, *J* = 7.6 Hz, 2H, ArH), 7.64−7.61 (m, 3H, ArH), 7.56−7.54 (m, 2H, ArH), 7.51−7.48 (m, 2H, ArH), 7.45 (d, *J* = 7.1 Hz, 1H, ArH), 7.41−7.36 (m, 3H, ArH), 4.19 (d, *J* = 13.6 Hz, 1H, CgP), 2.20 (d, *J* = 13.9 Hz, 1H, CgP), 1.85 (d, *J* = 13.7 Hz, 2H, CgP), 1.61 (s, 3H, Me), 1.57 (s, 3H, Me), 1.52−1.51 (m, 6H, Me). $^{13}C\{^1H\}$ NMR (125.8 MHz, $CDCl_3$): δ 144.1 (ArC), 137.7 (ArC), 135.0 (ArC), 134.8 (ArC), 134.5 (ArC), 133.9 (ArC), 133.0 (ArC), 132.7 (ArC), 132.4 (ArC), 132.1 (ArC), 131.6 (ArC), 129.1 (ArC), 128.7 (ArC), 128.4 (ArC), 97.6 (CgP), 97.0 (CgP), 79.3 (CgP), 74.8 (CgP), 41.7 (CgP), 40.4 (CgP), 28.6 (Me), 27.8 (Me), 26.9 (Me), 25.7 (Me). $^{31}P\{^1H\}$ NMR (202.5 MHz, $CDCl_3$): no observable signals in the $^{31}P\{^1H\}$ NMR spectrum. Anal. Calcd for $C_{28}H_{30}Cl_2NiO_3P_2$: C, 55.49; H, 4.99; N, 0. Found: C, 55.16; H, 5.21; N, <0.3.

Synthesis of (L16)$NiCl_2$. In a nitrogen-filled glovebox, a 4 dram vial containing a magnetic stir bar was charged with $NiCl_2$(dme) (48.9 mg, 0.223 mmol, 1.0 equiv) and **L16** (150.0 mg, 0.268 mmol, 1.2 equiv). The solid mixture was dissolved in THF (ca. 2 mL),

DOI: 10.1021/acs.organomet.8b00605
Organometallics XXXX, XXX, XXX−XXX

magnetic stirring was initiated, and the resulting solution was stirred at room temperature for 16 h. The crude reaction mixture was directly poured into a glass frit that was then washed thoroughly with pentane (5 × 5 mL). The product was collected by passing CH_2Cl_2 (ca. 25 mL) through the frit, followed by evaporation of solvent from the eluent. The product was then dried in vacuo to afford the desired complex as a dark purple solid (145 mg, 94%). A single crystal suitable for X-ray diffraction was prepared by slow evaporation of a cold (0 °C) CH_2Cl_2 solution of (**L16**)$NiCl_2$. The ^{1}H NMR features of this compound were sufficiently broad as to preclude meaningful interpretation, and no signals were observed in the $^{31}P\{^1H\}$ NMR spectrum. Anal. Calcd for $C_{34}H_{42}Cl_2NiO_3P_2$: C, 59.14; H, 6.14; N, 0. Found: C, 59.32; H, 6.11; N, < 0.3.

Crystallographic Solution and Refinement Details. Crystallographic data were obtained at or below 193(2) K on a Bruker D8/APEX II CCD diffractometer equipped with a CCD area detector, employing samples that were mounted in inert oil and transferred to a cold gas stream on the diffractometer. Data reduction, correction for Lorentz−polarization, and absorption correction were each performed. Structure solution and least-squares refinement on F^2 were used throughout. All non-hydrogen atoms were refined with anisotropic displacement parameters. Full crystallographic solution and refinement details are provided in the deposited CIF files (1858791 and 1858792).

General Computational Information. Geometry optimizations and frequency calculations were performed on all species with the B3LYP functional[25,26] and the XDM[27,28] dispersion correction. A mixed basis set was used, consisting of 6-31G* for C and H and 6-31+G* for all other elements. Single-point energy calculations on the optimized geometries were carried out using the same B3LYP-XDM method with the 6-311+G(2d,2p) basis set. The XDM damping parameters were a_1 = 0 Å and a_2 = 3.7737 Å for the geometry optimizations and a_1 = 0.4376 Å and , a_2 = 2.1607 Å for the single-point energies. All calculations were performed using the Gaussian 09[38] software package, along with the postg program for the dispersion energies. NCI plots[30] were generated using the B3LYP/6-311+G(2d,2p) wave functions via the NCIPLOT program.[39] Interactions between only the incipient $PhNH_2$ moiety and the ancillary ligand are shown and are represented using a 0.5 au reduced gradient isosurface. The postg and NCIPLOT programs can be downloaded from http://schooner.chem.dal.ca.

■ ASSOCIATED CONTENT

Supporting Information

The Supporting Information is available free of charge at the ACS Publications Web site. (PDF). The Supporting Information is available free of charge on the ACS Publications website at DOI: 10.1021/acs.organomet.8b00605.

Reaction progress data and compound characterization data, including NMR spectra (PDF)

Accession Codes

CCDC 1858791−1858792 contain the supplementary crystallographic data for this paper. These data can be obtained free of charge via www.ccdc.cam.ac.uk/data_request/cif, or by emailing data_request@ccdc.cam.ac.uk, or by contacting The Cambridge Crystallographic Data Centre, 12 Union Road, Cambridge CB2 1EZ, UK; fax: +44 1223 336033.

■ AUTHOR INFORMATION

Corresponding Authors

*E-mail for E.R.J.: erin.johnson@dal.ca.

*E-mail for M.S.: mark.stradiotto@dal.ca.

ORCID

Michael J. Ferguson: 0000-0002-5221-4401

Erin R. Johnson: 0000-0002-5651-468X

Mark Stradiotto: 0000-0002-6913-5160

Notes

The authors declare the following competing financial interest(s): Dalhousie University has filed patents on the DalPhos ancillary ligands and derived nickel pre-catalysts used in this work, from which royalty payments may be derived.

■ ACKNOWLEDGMENTS

Operational funding for this work was provided by the Natural Sciences and Engineering Research Council of Canada (Discovery Grant RGPIN-2014-4807). We are grateful to the Natural Sciences and Engineering Research Council of Canada (Discovery Grants for M.S. and E.R.J.; CGS-D for C.M.L., and Vanier CGS for J.P.T.) and Dalhousie University for their support of this work. We acknowledge Compute Canada (ACEnet) for computational resources and thank Cytec/Solvay for a gift of CgPH. We also thank Dr. Michael Lumsden (NMR-3, Dalhousie) for ongoing technical assistance in the acquisition of NMR data and Mr. Xiao Feng (Maritime Mass Spectrometry Laboratories, Dalhousie) for technical assistance in the acquisition of mass spectrometric data.

■ REFERENCES

(1) Ruiz-Castillo, P.; Buchwald, S. L. Applications of Palladium-Catalyzed C−N Cross-Coupling Reactions. *Chem. Rev.* **2016**, *116*, 12564−12649.

(2) Schranck, J.; Rotzler, J. Valorization of the Primary Building Blocks Ammonia and Acetone Featuring Pd- and Ni-Catalyzed Monoarylations. *Org. Process Res. Dev.* **2015**, *19*, 1936−1943.

(3) Schranck, J.; Tlili, A. Transition-Metal-Catalyzed Monoarylation of Ammonia. *ACS Catal.* **2018**, *8*, 405−418.

(4) Cragg, G. M.; Grothaus, P. G.; Newman, D. J. Impact of Natural Products on Developing New Anti-Cancer Agents. *Chem. Rev.* **2009**, *109*, 3012−3043.

(5) Aubin, Y.; Fischmeister, C.; Thomas, C. M.; Renaud, J.-L. Direct Amination of Aryl Halides with Ammonia. *Chem. Soc. Rev.* **2010**, *39*, 4130−4145.

(6) Widenhoefer, R. A.; Buchwald, S. L. Formation of Palladium Bis(Amine) Complexes from Reaction of Amine with Palladium Tris(*o*-tolyl)Phosphine Mono(Amine) Complexes. *Organometallics* **1996**, *15*, 3534−3542.

(7) Klinkenberg, J. L.; Hartwig, J. F. Slow Reductive Elimination from Arylpalladium Parent Amido Complexes. *J. Am. Chem. Soc.* **2010**, *132*, 11830−11833.

(8) Surry, D. S.; Buchwald, S. L. Dialkylbiaryl Phosphines in Pd-Catalyzed Amination: A User's Guide. *Chem. Sci.* **2011**, *2*, 27−50.

(9) Shen, Q.; Hartwig, J. F. Palladium Catalyzed Coupling of Ammonia and Lithium Amide with Aryl Halides. *J. Am. Chem. Soc.* **2006**, *128*, 10028−10029.

(10) Cheung, C. W.; Surry, D. S.; Buchwald, S. L. Mild and Highly Selective Palladium-Catalyzed Monoarylation of Ammonia Enabled by the Use of Bulky Biarylphosphine Ligands and Palladacycle Precatalysts. *Org. Lett.* **2013**, *15*, 3734−3737.

(11) Lundgren, R. J.; Peters, B. D.; Alsabeh, P. G.; Stradiotto, M. A P,N-Ligand for Palladium-Catalyzed Ammonia Arylation: Coupling of Deactivated Aryl Chlorides, Chemoselective Arylations, and Room Temperature Reactions. *Angew. Chem., Int. Ed.* **2010**, *49*, 4071−4074.

(12) Alsabeh, P. G.; Lundgren, R. J.; McDonald, R.; Seechurn, C. C. C. J.; Colacot, T. J.; Stradiotto, M. An Examination of the Palladium/Mor-DalPhos Catalyst System in the Context of Selective Ammonia Monoarylation at Room Temperature. *Chem. - Eur. J.* **2013**, *19*, 2131−2141.

(13) Alsabeh, P. G.; McDonald, R.; Stradiotto, M. Stoichiometric Reactivity Relevant to the Mor-Dalphos/Pd-Catalyzed Cross-Coupling of Ammonia and 1-Bromo-2-(Phenylethynyl)Benzene. *Organometallics* **2012**, *31*, 1049−1054.

(14) Crawford, S. M.; Lavery, C. B.; Stradiotto, M. BippyPhos: A Single Ligand With Unprecedented Scope in the Buchwald−Hartwig

DOI: 10.1021/acs.organomet.8b00605
Organometallics XXXX, XXX, XXX−XXX

Amination of (Hetero)aryl Chlorides. *Chem. - Eur. J.* **2013**, *19*, 16760−16771.
(15) Lombardi, C.; Day, J.; Chandrasoma, N.; Mitchell, D.; Rodriguez, M. J.; Farmer, J. L.; Organ, M. G. Selective Cross-Coupling of (Hetero)Aryl Halides with Ammonia to Produce Primary Arylamines Using Pd-NHC Complexes. *Organometallics* **2017**, *36*, 251−254.
(16) While the copper-catalyzed cross-coupling of (hetero)aryl chlorides with ammonia is generally ineffective, selected examples of such transformations have been reported: Fan, M. Y.; Zhou, W.; Jiang, Y. W.; Ma, D. W. Assembly of Primary (Hetero)Arylamines Via CuI/Oxalic Diamide-Catalyzed Coupling of Aryl Chlorides and Ammonia. *Org. Lett.* **2015**, *17*, 5934−5937.
(17) Marín, M.; Rama, R. J.; Nicasio, M. C. Ni-Catalyzed Amination Reactions: An Overview. *Chem. Rec.* **2016**, *16*, 1819−1832.
(18) Lavoie, C. M.; Stradiotto, M. Bisphosphines: A Prominent Ancillary Ligand Class for Application in Nickel-Catalyzed C−N Cross-Coupling. *ACS Catal.* **2018**, *8*, 7228−7250.
(19) Borzenko, A.; Rotta-Loria, N. L.; MacQueen, P. M.; Lavoie, C. M.; McDonald, R.; Stradiotto, M. Nickel-Catalyzed Monoarylation of Ammonia. *Angew. Chem., Int. Ed.* **2015**, *54*, 3773−3777.
(20) Green, R. A.; Hartwig, J. F. Nickel-Catalyzed Amination of Aryl Chlorides with Ammonia or Ammonium Salts. *Angew. Chem., Int. Ed.* **2015**, *54*, 3768−3772.
(21) Lavoie, C. M.; MacQueen, P. M.; Rotta-Loria, N. L.; Sawatzky, R. S.; Borzenko, A.; Chisholm, A. J.; Hargreaves, B. K. V.; McDonald, R.; Ferguson, M. J.; Stradiotto, M. Challenging Nickel-Catalysed Amine Arylations Enabled by Tailored Ancillary Ligand Design. *Nat. Commun.* **2016**, *7*, 11073.
(22) Lavoie, C. M.; MacQueen, P. M.; Stradiotto, M. Nickel-Catalyzed N-Arylation of Primary Amides and Lactams with Activated (Hetero)Aryl Electrophiles. *Chem. - Eur. J.* **2016**, *22*, 18752−18755.
(23) Lavoie, C. M.; McDonald, R.; Johnson, E. R.; Stradiotto, M. Bisphosphine-Ligated Nickel Pre-Catalysts in C(sp^2)−N Cross-Couplings of Aryl Chlorides: A Comparison of Nickel(I) and Nickel(II). *Adv. Synth. Catal.* **2017**, *359*, 2972−2980.
(24) Gatien, A. V.; Lavoie, C. M.; Bennett, R. N.; Ferguson, M. J.; McDonald, R.; Johnson, E. R.; Speed, A. W. H.; Stradiotto, M. Application of Diazaphospholidine/Diazaphospholene-Based Bisphosphines in Room-Temperature Nickel-Catalyzed C(sp^2)−N Cross-Couplings of Primary Alkylamines with (Hetero)Aryl Chlorides and Bromides. *ACS Catal.* **2018**, *8*, 5328−5339.
(25) Lee, C.; Yang, W.; Parr, R. G. Development of the Colle-Salvetti Correlation-Energy Formula into a Functional of the Electron Density. *Phys. Rev. B: Condens. Matter Mater. Phys.* **1988**, *37*, 785−789.
(26) Becke, A. D. Density-Functional Thermochemistry. III. The Role of Exact Exchange. *J. Chem. Phys.* **1993**, *98*, 5648−5652.
(27) Becke, A. D.; Johnson, E. R. Exchange-Hole Dipole Moment and the Dispersion Interaction Revisited. *J. Chem. Phys.* **2007**, *127*, 154108.
(28) Otero-de-la-Roza, A.; Johnson, E. R. Non-Covalent Interactions and Thermochemistry Using XDM-Corrected Hybrid and Range-Separated Hybrid Density Functionals. *J. Chem. Phys.* **2013**, *138*, 204109.
(29) Clark, J. S. K.; McGuire, R. T.; Lavoie, C. M.; Ferguson, M. J.; Stradiotto, M. Examining the Impact of Heteroaryl Variants of PAd-DalPhos on Nickel-Catalyzed C(sp^2)-N Cross-Couplings. *Organometallics* **2018**, DOI: 10.1021/acs.organomet.8b00451.
(30) Johnson, E. R.; Keinan, S.; Mori-Sánchez, P.; Contreras-García, J.; Cohen, A. J.; Yang, W. Revealing Noncovalent Interactions. *J. Am. Chem. Soc.* **2010**, *132*, 6498−6506.
(31) Nielsen, M. C.; Bonney, K. J.; Schoenebeck, F. Computational Ligand Design for the Reductive Elimination of $ArCF_3$ from a Small Bite Angle Pd^{II} Complex: Remarkable Effect of a Perfluoroalkyl Phosphine. *Angew. Chem., Int. Ed.* **2014**, *53*, 5903−5906.
(32) Yin, G.; Kalvet, I.; Englert, U.; Schoenebeck, F. Fundamental Studies and Development of Nickel-Catalyzed Trifluoromethylthiolation of Aryl Chlorides: Active Catalytic Species and Key Roles of Ligand and Traceless MeCN Additive Revealed. *J. Am. Chem. Soc.* **2015**, *137*, 4164−4172.
(33) Hazari, N.; Melvin, P. R.; Beromi, M. M. Well-Defined Nickel and Palladium Precatalysts for Cross-Coupling. *Nat. Rev. Chem.* **2017**, *1*, 0025.
(34) Standley, E. A.; Jamison, T. F. Simplifying Nickel(0) Catalysis: An Air-Stable Nickel Precatalyst for the Internally Selective Benzylation of Terminal Alkenes. *J. Am. Chem. Soc.* **2013**, *135*, 1585−1592.
(35) MacQueen, P. M.; Stradiotto, M. Nickel-Catalyzed Cross-Coupling of Ammonia or Primary Alkylamines with (Hetero)Aryl Sulfamates, Carbamates, or Pivalates. *Synlett* **2017**, *28*, 1652−1656.
(36) Schranck, J.; Furer, P.; Hartmann, V.; Tlili, A. Nickel-Catalyzed Amination of Aryl Carbamates with Ammonia. *Eur. J. Org. Chem.* **2017**, *2017*, 3496−3500.
(37) Clark, J. S. K.; Lavoie, C. M.; MacQueen, P. M.; Ferguson, M. J.; Stradiotto, M. A Comparative Reactivity Survey of Some Prominent Bisphosphine Nickel(II) Precatalysts in C−N Cross-Coupling. *Organometallics* **2016**, *35*, 3248−3254.
(38) Frisch, M. J., et al. *Gaussian 09, Revision B.01*; Gaussian, Inc., Wallingford, CT, 2010.
(39) Contreras-García, J.; Johnson, E. R.; Keinan, S.; Chaudret, R.; Piquemal, J.-P.; Beratan, D. N.; Yang, W. NCIPLOT: A Program for Plotting Noncovalent Interaction Regions. *J. Chem. Theory Comput.* **2011**, *7*, 625−632.

DOI: 10.1021/acs.organomet.8b00605
Organometallics XXXX, XXX, XXX−XXX